

## Intermediate spin state of $\text{Co}^{3+}$ and $\text{Co}^{4+}$ ions in $\text{La}_{0.5}\text{Ba}_{0.5}\text{CoO}_3$ evidenced by Jahn-Teller distortions

F. Fauth,<sup>1,\*</sup> E. Suard,<sup>2</sup> and V. Caignaert<sup>3</sup>

<sup>1</sup>European Synchrotron Radiation Facility, 6, Rue Jules Horowitz, B.P. 220, 38043 Grenoble Cedex, France

<sup>2</sup>Institut Laue Langevin, 6, Rue Jules Horowitz, B.P. 156X, 38042 Grenoble Cedex 9, France

<sup>3</sup>Laboratoire CRISMAT/ISMRA, Boulevard du M<sup>al</sup> Juin, 14050 Caen Cedex, France

(Received 27 September 2001; published 28 December 2001)

From high resolution neutron and synchrotron powder diffraction studies performed on the ideal cubic perovskite compound  $\text{La}_{0.5}\text{Ba}_{0.5}\text{CoO}_3$ , we have observed the onset of a long-range tetragonal phase accompanying a para-ferromagnetic transition at  $T_C \sim 180$  K. The lowering of the crystal symmetry is the direct signature of a cooperative and static Jahn-Teller (JT) distortion of the  $\text{CoO}_6$  octahedra. The JT effect is favored by the intermediate spin-state configuration,  $t_{2g}^5 e_g^1$  and  $t_{2g}^5 e_g^1 L$ , of the  $\text{Co}^{3+}$  ( $d^6$ ) and  $\text{Co}^{4+}$  ( $d^5$ ) species occurring in the structure. At  $T_C$ , the material exhibits a sudden increase of metallicity and a substantial peak in the magnetoresistivity. When further cooling down, the gradual ordering of the  $d_{3z^2-r^2}$  orbitals leads to a metal-insulator-like transition at  $T_{MI} \sim 120$  K.

DOI: 10.1103/PhysRevB.65.060401

PACS number(s): 75.30.Vn, 61.12.-q, 71.30.+h, 75.25.+z

Perovskite-like oxides of formula  $A_{1-x}A'_xBO_3$  ( $A$  is a trivalent lanthanide,  $A'$  a divalent alkaline, and  $B$  a  $3d$  transition metal) have always attracted considerable interest because of their fascinating physical properties. The last decade was marked by the discovery of colossal magnetoresistivity (CMR) in manganates which led to an extensive (re-) investigation of  $B = \text{Mn}, \text{Co},$  and  $\text{Ni}$  systems. Here, we present diffraction and transport properties measurements performed on  $\text{La}_{0.5}\text{Ba}_{0.5}\text{CoO}_3$ . This compound is a particular case of the more general family of layered perovskite-based systems  $L\text{BaCo}_2\text{O}_{5+\delta}$  ( $L = \text{lanthanide}, 0 \leq \delta \leq 1$ ) which have been subject of increasing number of studies recently.<sup>1</sup> Mainly since highest magnetoresistivity (MR) ratios ever observed in Co-based oxides have been reported in  $L\text{BaCo}_2\text{O}_{5.4}$  ( $L = \text{Eu}, \text{Gd}$ ).<sup>2</sup> In their stoichiometric form,  $\delta = 1$ ,  $L\text{BaCo}_2\text{O}_{5+\delta}$  joins the class of perovskite-like oxides and is therefore related to  $\text{LaCoO}_3$  and its hole-doped derivatives  $\text{La}_{1-x}A'_x\text{CoO}_3$ ,  $A' = \text{Ca}, \text{Sr}, \text{Ba}$ . These latter compounds are particularly intriguing since they display several changes in their electronic and magnetic properties as function of temperature<sup>3</sup> and/or divalent substitution.<sup>4</sup> The rich magnetic and electronic phase diagram of  $\text{LaCoO}_3$  results from the close values of the crystal field splitting,  $\Delta_{cf}$ , and of the exchange energy,  $\Delta_{ex}$ , for  $\text{Co}^{3+}$  ( $3d^6$ ) ions in octahedral environment. Thus, either the low-spin (LS) ( $t_{2g}^6 e_g^0, S=0$ ) or the intermediate-spin (IS) ( $t_{2g}^5 e_g^1, S=1$ ) configuration appears energetically more favorable than the Hund's rule predicted high-spin (HS) state ( $t_{2g}^4 e_g^2, S=2$ ).<sup>5</sup> In the hole-doped compounds,  $\text{La}_{1-x}A'_x\text{CoO}_3$ , the complexity of the system is further increased by the occurrence of  $\text{Co}^{4+}$  ( $3d^5$ ) ions which are susceptible to exist in several spin-state configurations as well.<sup>6-8</sup>

The several possible electronic configurations of cobalt ions in  $\text{La}_{1-x}A'_x\text{CoO}_3$  are generally either indirectly inferred from magnetic and/or transport properties measurements<sup>3,4</sup> or predicted from density functional calculations.<sup>5-8</sup> Alternatively, electron and/or x-ray spectroscopy studies allow a deeper understanding of this problem, particularly in stress-

ing out the strong hybridization of Co ions in octahedral environment.<sup>7,8</sup> Although appearing as the best tools for probing electronic configurations of transition metal elements, soft x-ray spectroscopic techniques are unfortunately not applicable in our case because of coinciding Ba and Co absorption edges. On the other hand, the impact of the electronic configuration on the crystal structure, although non-negligible, appears much weaker and is therefore hardly detectable experimentally. For example, although displaying successive magnetic and electronic transitions up to 1250 K,  $\text{LaCoO}_3$  does not exhibit relevant structural phase transition as was clearly stated from latest neutron diffraction measurements<sup>9</sup> which, however, partially contradicted previous x-ray studies.<sup>10</sup> Note that the reported structural transitions,  $R\bar{3}c \rightleftharpoons R\bar{3}$ , mainly focused on the possible (alternatively dynamical short-range or static long-range) ordering of  $\text{LS-Co}^{III}$  and  $\text{HS-Co}^{3+}$  species coexisting at selected temperatures.

In order to explain the strength of the observed magnetic moments, the assumption was made that the  $\text{IS-Co}^{3+}$  state might also be present in  $\text{La}_{1-x}A'_x\text{CoO}_3$ . Goodenough initially developed this hypothesis within an itinerant  $3d$  electron picture.<sup>11</sup> Recently, Korotin *et al.* concluded from  $\text{LDA}+U$  calculations to a stable IS ground state above a critical Co-O bond length.<sup>5</sup> Moreover, this IS configuration can alternatively develop an orbital ordered phase leading to a nonmetallic state (gapless semiconductor). Since the  $\text{IS-Co}^{3+}$ , but  $\text{IS-Co}^{4+}$  ( $t_{2g}^4 e_g^1$ ) as well, are expected to be strong Jahn-Teller (JT) ions, assessment on the electronic configuration of the cobalt ions in  $\text{La}_{1-x}A'_x\text{CoO}_3$  could also be done from the observation of an hypothetical JT-induced distortion. So far, only *isolated local* tetragonal distortions have been observed in such systems by electron microscopy<sup>12</sup> or infrared spectroscopy.<sup>13</sup> Here, we report on the onset of a *long-range* tetragonal phase below  $T_C \sim 180$  K in  $\text{La}_{0.5}\text{Ba}_{0.5}\text{CoO}_3$ . The ferrodistorptive transition results from the cooperative static Jahn-Teller distortion of the  $\text{CoO}_6$  octahedra which appears only possible when assuming

$\text{Co}^{3+}$  and  $\text{Co}^{4+}$  ions in intermediate spin state. This picture is supported by the magnetic structure and the thermal dependence of the resistivity.

The  $\text{La}_{0.5}\text{Ba}_{0.5}\text{CoO}_3$  sample was synthesized using the same method as described in Ref. 14 to produce  $\text{LaBaMn}_2\text{O}_{5+\delta}$  ( $\delta=0,1$ ). Here, however, we additionally annealed the sample under 100 bars  $\text{O}_2$  atmosphere. The oxygen stoichiometry of our sample was found to be  $3.000 \pm 0.005$  from Rietveld refinement of room temperature neutron powder diffraction data. The crystallographic structure in the temperature range 1.5–300 K was determined using high-resolution neutron (NPD) and synchrotron (SPD) powder diffraction techniques. High-resolution NPD data were collected on the diffractometer D2B ( $\lambda=1.594$  Å) of the Institute Laue-Langevin (ILL) in Grenoble. SPD measurements were performed at the European Synchrotron Radiation Facility (ESRF) in Grenoble on BM16 ( $\lambda=0.4912$  Å,  $\lambda=0.5985$  Å) and the Swiss-Norwegian beamline ( $\lambda=0.6004$  Å). The magnetic properties of  $\text{La}_{0.5}\text{Ba}_{0.5}\text{CoO}_3$  were followed from both NPD data collected on the high-intensity diffractometer D1B of the ILL ( $\lambda=2.52$  Å) and from magnetization measurement using a vibrating magnetometer. Electrical resistance was measured down to 4 K without and with the application of an external magnetic field of 7 T on a standard PPMS equipment.

The RT crystallographic structure of  $\text{La}_{0.5}\text{Ba}_{0.5}\text{CoO}_3$  appears incredibly simple since it can be refined using the cubic perovskite model of cell parameter  $a_p=3.8843$  Å [space group (S.G.)  $Pm\bar{3}m$ , isotropic displacement parameters in Å<sup>2</sup>:  $B_{\text{La/Ba}}=0.42$ ,  $B_{\text{Co}}=0.27$ ,  $B_{\text{O}}=1.20$ , reliability factor  $R_B=2.8\%$ ] (Fig. 1). Alternatively, these data can be refined using the low-temperature phase model explained below [S.G.  $P4/mmm$ ,  $(c-a)/a\sim 0.07\%$ ] or using the same rhombohedral distorted cell (S.G.  $R\bar{3}c$ ,  $a=\sqrt{2}a_p$ ,  $\alpha\sim 60.0$ ) as observed in  $\text{La}_{1-x}\text{A}'_x\text{CoO}_3$  ( $\text{A}'=\text{Ca,Sr,Ba}$ ;  $x<0.4$ ), but without significant increase in the quality of the fit. Thus, according to the usage, we keep the model with the highest symmetry and the smallest unit cell. The  $Pm\bar{3}m$  crystallographic structure means first of all that both La and Ba ions are statistically distributed on the body center site, whereas Co ions are embedded at the center of the regular octahedron formed by its six neighboring oxygen ions. None of the characteristic tilting or distortions of the  $\text{CoO}_6$  octahedra susceptible to occur in perovskites has been evidenced experimentally. Referring to previous reports on  $\text{La}_{1-x}\text{A}'_x\text{CoO}_3$  [ $\text{A}'=\text{Ca}$  (Ref. 15),  $\text{Sr}$  (Ref. 6),  $\text{Ba}$  (Ref. 16)], the observed (undistorted) cubic structure is explained by the large mean ionic radius of the  $\text{La}_{0.5}\text{Ba}_{0.5}$  ions occupying the body center site.

At the lowest measured temperatures, we noticed a splitting of selected peaks which could be exclusively accounted for by a long-range tetragonal distortion (S.G.  $P4/mmm$  with cell parameters  $a=3.8683$  Å,  $c=3.8748$  Å,  $B_{\text{La/Ba}}=0.10$ ,  $B_{\text{Co}}=0.18$ ,  $B_{\text{O}_1}=0.84$ ,  $B_{\text{O}_2}=0.96$ ,  $R_B=2.3\%$ ) (Fig. 1). Compared to the cubic phase, the  $P4/mmm$  symmetry differs only in the splitting of the oxygen position,  $(0,0,\frac{1}{2}) \rightarrow (0,0,\frac{1}{2}) + (0,\frac{1}{2},0)$ , but keeps a unique site for the Co ion.

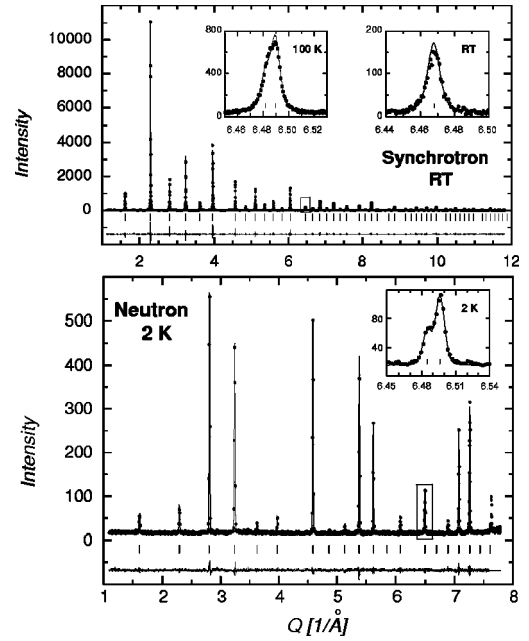


FIG. 1. Synchrotron (top) and neutron (bottom) diffraction patterns of  $\text{La}_{0.5}\text{Ba}_{0.5}\text{CoO}_3$ . In the inset, we have magnified the 004/400 Bragg reflection region at selected temperatures. The points and the line refer to measurements and calculation (including ferromagnetism in the neutron case), the bottom line represents the difference. Data are refined in space group  $Pm\bar{3}m$  at RT,  $P4/mmm$  otherwise.

This LT phase originates from the elongation of the  $\text{CoO}_6$  octahedra along the unique axis  $c$  (ferrodistortive structure) and in no way from the ordering of the La and Ba ions. Contrary to what happens in the layered cobaltates  $\text{LaBaCo}_2\text{O}_5$  (Ref. 1) or in some temperature regions of  $\text{LaCoO}_3$ ,<sup>9,10</sup> the new crystal structure is not attributed to the long-range ordering of the two Co species existing in  $\text{La}_{0.5}\text{Ba}_{0.5}\text{CoO}_3$ .

As can be seen in Fig. 2, the onset of the crystallographic distortion coincides with the onset of long-range ferromagnetic ordering of the Co moments at  $T_C\sim 180$  K. At 2 K, the saturation moment value amounts to  $1.9\mu_B/\text{Co}$ . At 2 K, the small tetragonal distortion does not allow one to distinguish the exact orientation of the magnetic moments from Rietveld refinement. We thus assumed in our calculations the moments pointing along the unique axis direction. Transport properties measurements performed on  $\text{La}_{0.5}\text{Ba}_{0.5}\text{CoO}_3$  from 350 K down to 4 K clearly determine three temperature regions (see Fig. 3). Above  $T_C$ , the material exhibits a semi-metallic behavior with a sudden increase of the electric conductivity at  $T_C$ . This change coincides with a maximum of the negative magnetoresistance and is explained by Zener's double-exchange mechanism.<sup>17</sup> Although reduced compared to the manganates or the layered cobaltates, the actual peak value in the MR ratio is of the same order as the highest ratio ever observed in Co-based oxides  $\text{La}_x\text{A}'_{1-x}\text{CoO}_3$ .<sup>18</sup> When further cooling down,  $\text{La}_{0.5}\text{Ba}_{0.5}\text{CoO}_3$  displays a metal-insulator-like transition at  $T_{MI}\sim 120$  K accompanied by an upturn of the MR ratio. At this stage, it is worth pointing out

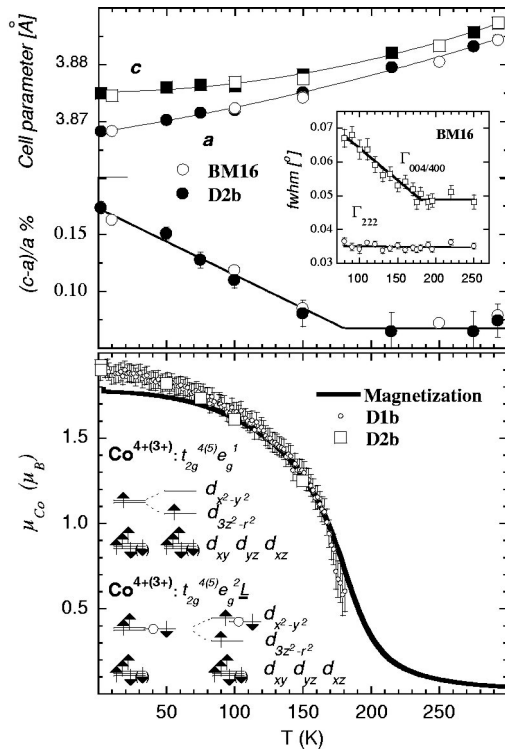


FIG. 2. Thermal dependence of the cell parameters (also corresponding to two times Co-O distances) (top), the tetragonal distortion (mid), and the magnetic moment per Co ions (bottom) in  $\text{La}_{0.5}\text{Ba}_{0.5}\text{CoO}_3$ . In the inset, we have compared the peak width of selected reflections (a splitting and a not-splitting one in  $P4/mmm$ ). In the bottom part, we have drawn the electronic configurations of the Co species occurring above and below the JT transition.

that although of insulating character, the residual resistivity remains very low at 4 K and the material is more likely to be described as a semiconductor.

From above experimental results, the most notable features of  $\text{La}_{0.5}\text{Ba}_{0.5}\text{CoO}_3$  are the long-range tetragonal structure below  $T_C$  and the metal-semiconductor transition at  $T_{MI} \sim 120$  K. The ferromagnetic structure essentially agrees with measurements already reported for  $\text{La}_{0.5}\text{Ba}_{0.5}\text{CoO}_3$ ,

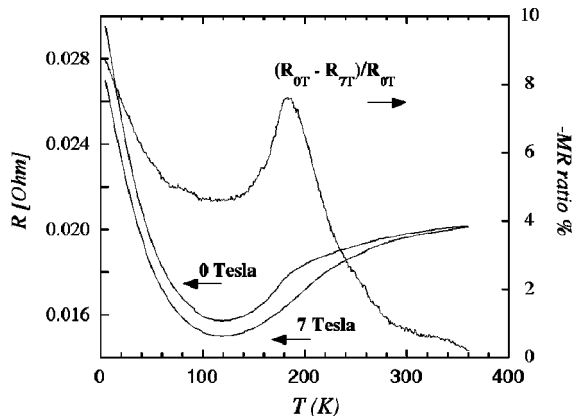


FIG. 3. Thermal dependence of the resistivity measured in  $\text{La}_{0.5}\text{Ba}_{0.5}\text{CoO}_3$  with and without an external magnetic field and the corresponding negative magnetoresistive ratio.

with perhaps a smaller  $T_C$  in our case.<sup>19</sup> In variance to most of the previous studies, we report here an ideal cubic perovskite structure at RT which is doubly justified by the large mean ionic radius of the body center site and the high angular resolution of the instruments used. As deduced from the stoichiometry of  $\text{La}_{0.5}\text{Ba}_{0.5}\text{CoO}_{3.00}$ , the Co ions exist with equal ratio in 3+ and 4+ valence state ( $3d^6$  and  $3d^5$  configuration, respectively). Quantitatively, the magnetic moment value at saturation,  $1.9\mu_B/\text{Co}$ , precludes the Hund's rule predicted high-spin state for all Co species (HS- $\text{Co}^{3+}$ :  $t_{2g}^4 e_g^2, S=2$ ; HS- $\text{Co}^{4+}$ :  $t_{2g}^3 e_g^2, S=5/2$ ) which would result in a spin-only magnetic contribution of  $4.5\mu_B/\text{Co}$ . More generally, within a pure ionic model the observed magnetization can only be accounted for assuming at least one of the Co species in an intermediate-spin (IS) state. Since IS configurations have the twofold degenerate  $e_g$ -type ( $d_{3z^2-r^2}/d_{x^2-y^2}$ ) orbitals singly occupied, they further appear favorable to the occurrence of Jahn-Teller distortions of the  $\text{CoO}_6$  octahedra. However, following Goodenough-Kanamori rules of superexchange, singly occupied  $e_g$  orbitals tend to favor strong antiferromagnetic coupling in perovskite structure.<sup>20</sup>

At this point, we have to count with possible hybridization of the Co-3d and O-2p orbitals which is known to be non-negligible in Co-based perovskite, and even stronger for IS or LS states. Typically, from x-ray and/or electron absorption spectroscopy studies performed in  $\text{La}_{1-x}\text{Sr}_x\text{CoO}_3$  ( $x=0,1$ ), the electronic ground state turned out to be in majority  $d^7\bar{L}$  and  $d^6\bar{L}$  for  $\text{Co}^{3+}$  ( $d^6$ ) and  $\text{Co}^{4+}$  ( $d^5$ ), respectively.<sup>7,8</sup> Hence, when properly considering covalency effects, we can give the following qualitative and simplified electronic picture to explain the experimental evidences reported in  $\text{La}_{0.5}\text{Ba}_{0.5}\text{CoO}_3$ . We assume the  $\text{Co}^{3+}$  and  $\text{Co}^{4+}$  ions to exist as  $\alpha|d^6\rangle + \beta|d^7\bar{L}\rangle$  and  $\alpha'|d^5\rangle + \beta'|d^6\bar{L}\rangle$  states, respectively. For both ions, the nonhybridized configuration are IS states whereas the hybridized configuration can be seen as the corresponding HS state but with, coupled to electrons of  $e_g$  symmetry, a hole of corresponding symmetry on the oxygen  $p_\sigma$  orbital. (see inset in Fig. 2). Over the complete measured temperature range, the magnetic and transport properties follow a mechanism similar to Zener's double exchange, meaning ferromagnetic exchange interactions and electric conduction by  $e_g$ -electron hopping between Co sites.<sup>17</sup> Indeed, in order for an oxygen hole of  $e_g$  symmetry to hybridize with both adjacent Co ions, the spin of the  $e_g$  electrons on both Co ions should be parallel. Note that double exchange type interactions also discard the occurrence of charge ordering which is in agreement with our observations. At  $T_C$ , the ordering of the Co magnetic moments reduces the spin-disorder scattering, increasing thus the electric conductivity. The application of a magnetic field reduces spin fluctuations and leads therefore to the observed negative magnetoresistance. Also at  $T_C$ , the gap between  $d_{3z^2-r^2}$ - and  $d_{x^2-y^2}$ -type orbitals opens owing to the Jahn-Teller effect. Above  $T_{MI}$ , thermal fluctuations allow occupation of both  $e_g$ -type orbitals. When further cooling down, population of the  $d_{3z^2-r^2}$ -type orbitals of lower energy gradually increases, which is experimentally reflected by the continuous increase

of the  $\text{CoO}_6$  distortion parameter. This smooth increase is accompanied at  $T_{MI}$  by a change in the resistivity behavior. This temperature corresponds to a threshold where the opening of the gap is large enough for the ground state to be considered as partially orbitally ordered. Hence, the number of conduction channels by  $d_{x^2-y^2}$ -type electron hopping is reduced accordingly leading to a reduction of the electric conductivity.

In conclusion, we have experimentally evidenced the onset of a Jahn-Teller induced long range tetragonal phase below  $T_C \sim 180$  K in the exact stoichiometric compound  $\text{La}_{0.5}\text{Ba}_{0.5}\text{CoO}_{3.00}$ . Contrary to most of the parent  $\text{La}_{1-x}\text{A}_x\text{CoO}_3$  compounds, the distortion sets in within an ideal cubic perovskite structure rendering the JT effect more

spectacular since leading to a crystallographic phase transition. The occurrence of a metal-insulator-like transition at  $T_{MI} \sim 120$  K supports the LDA+ $U$  calculations performed by Korotin *et al.* suggesting the existence of two orbitally polarized magnetic solutions corresponding to IS states (one of them is a gapless semiconductor and the other is a metal).<sup>5</sup> In view of the actual results, closer reinvestigations of the low-temperature crystal structure of  $\text{La}_{1-x}\text{A}_x\text{CoO}_3$  systems by means of today's improved angular-resolution diffraction techniques appear desirable.

Experimental assistance from the staff of the Swiss-Norwegian Beam Lines at ESRF is gratefully acknowledged for part of the work done under contribution No. 01-01-233.

\*Email address: fauth@esrf.fr

<sup>1</sup>F. Fauth, E. Suard, V. Caignaert, B. Domengès, I. Mirebeau, and L. Keller, *Eur. Phys. J. B* **21**, 163 (2001), and references therein.

<sup>2</sup>C. Martin, A. Maignan, D. Pelloquin, N. Nguyen, and B. Raveau, *Appl. Phys. Lett.* **71**, 1421 (1997).

<sup>3</sup>M. Senaris-Rodriguez and J. Goodenough, *J. Solid State Chem.* **116**, 224 (1995), and references therein.

<sup>4</sup>M. Senaris-Rodriguez and J. Goodenough, *J. Solid State Chem.* **118**, 323 (1995), and references therein.

<sup>5</sup>M. Korotin, S. Ezhov, I. Solovyev, V. Anisimov, D. Khomskii, and G. Sawatzky, *Phys. Rev. B* **54**, 5309 (1996).

<sup>6</sup>P. Ravindran, P. Korzhavyi, H. Fjellvag, and A. Kjekhus, *Phys. Rev. B* **60**, 16 423 (1999).

<sup>7</sup>A. Chainani, M. Mathew, and D. Sarma, *Phys. Rev. B* **46**, 9976 (1992).

<sup>8</sup>R. Potze, G. Sawatzky, and M. Abbate, *Phys. Rev. B* **51**, 11 501 (1995).

<sup>9</sup>G. Thornton, B. Tofield, and A. Hewat, *J. Solid State Chem.* **61**, 301 (1986).

<sup>10</sup>P. Raccah and J. Goodenough, *Phys. Rev.* **155**, 932 (1967).

<sup>11</sup>J.B. Goodenough, *Mater. Res. Bull.* **6**, 967 (1971).

<sup>12</sup>Z. Wang and J. Zhang, *Phys. Rev. B* **54**, 1153 (1996).

<sup>13</sup>S. Yamaguchi, Y. Okimoto, and Y. Tokura, *Phys. Rev. B* **55**, R8666 (1997).

<sup>14</sup>F. Millange, V. Caignaert, B. Domengès, and B. Raveau, *Chem. Mater.* **10**, 1974 (1998).

<sup>15</sup>H. Taguchi, M. Shimada, and M. Koizumi, *J. Solid State Chem.* **41**, 329 (1982).

<sup>16</sup>S. Patil, H. Keer, and D. Chakrabarty, *Phys. Status Solidi A* **52**, 681 (1979).

<sup>17</sup>C. Zener, *Phys. Rev.* **81**, 440 (1950).

<sup>18</sup>R. Mahendiran, A. Raychaudhuri, A. Chainani, and D. Sarma, *J. Phys.: Condens. Matter* **7**, L561 (1995); R. Mahendiran and A. Raychaudhuri, *Phys. Rev. B* **54**, 16 044 (1996).

<sup>19</sup>I.O. Troyanchuk, N. Kasper, D.D. Khalyavin, H. Szymczak, R. Szymczak, and M. Baran, *Phys. Rev. B* **58**, 2418 (1998); Y. Moritomo, M. Takeo, X. Liu, T. Akimoto, and A. Nakamura, *ibid.* **58**, R13 334 (1998); P. Vanitha, A. Arulraj, P. Santosh, and C. Rao, *Chem. Mater.* **12**, 1666 (2000).

<sup>20</sup>J.B. Goodenough, *Phys. Rev.* **100**, 564 (1955); J. Kanamori, *J. Phys. Chem. Solids* **10**, 87 (1959).